Atomic physics

Sheldon Datz

Atomic Physics Division, Oak Ridge National Laboratory, Oak Ridge, Tennessee 37831

G. W. F. Drake

Department of Physics, University of Windsor, Ontario, Canada N9B 3P4

T. F. Gallagher

Department of Physics, University of Virginia, Charlottesville, Virginia 22901

H. Kleinpoppen

Atomic Physics Laboratory, University of Stirling, Stirling FK9 4LA, Scotland

G. zu Putlitz

Physikalisches Institut der Ruprecht-Karls-Universität Heidelberg, D-69120 Heidelberg, Germany

This Section contains examples of important areas in atomic physics, including articles on cold atoms collisions, accelerator-based atomic collisions, fundamental-type atomic collisions, high-precision atomic theory and the few-body problem, and ''exotic atoms.'' [S0034-6861(99)04502-X]

CONTENTS

I. INTRODUCTION[1]

Atomic physics deals with any interactions in nature in which the electromagnetic force plays a dominant role and the other forces of nature play relatively minor roles, or no roles at all. Even so these ''minor'' roles can be employed to great advantage to study a wide variety of subjects, such as the determination of nuclear properties, and even delve into quantum electrodynamics and parity nonconservation in weak interactions. Data from atomic physics are necessary inputs for modeling phenomena in plasmas, condensed matter, neutral fluids, etc. Ionized and neutral atoms, positive and negative electrons, physical properties of molecules, as opposed to chemical and biological, and exotic systems such as muonium and positronium can be considered to be fair game for this enormous field. Atomic physics is periodically reinvigorated by new experimental and theoretical methods. It led the way to initial developments in quantum mechanics and remains extraordinarily vigorous to this day. It is remarkable for its diversity. For example, its energy domain extends from nanokelvin temperatures to relativistic energies. It is also the proving ground for studying the border area between quantum and classical mechanics.

[1]The best single sourcebooks for research in atomic physics are the biennial proceedings of the International Conference on Atomic Physics (ICAP), for example, 1997, University of Windsor, Windsor, Ontario, Canada.

Atomic physics has its own unique dynamics, continuing as it began with the study of the electromagnetic spectra of ions, atoms, and molecules, over a spectrum now extended to all frequencies from radio waves to x-rays and gamma-rays and continuing, as well, with the study of processes involving collisions between neutral and charged atomic and molecular systems. The two strands of research inspired two classic treatises, *The Theory of Atomic Spectra* by E. U. Condon and G. H. Shortly (1935), and *The Theory of Atomic Collisions* by N. F. Mott and H. S. W. Massey (1965). The two strands intertwine and both have been transformed by the appearance of new tools, especially the laser. Dramatic advances in the range, sensitivity, and precision of experiments have occurred, particularly in the past one or two decades.[2] Because of the rapid increase in computational power, problems once set aside can now be attacked directly. For example, simulations and visualizations can be constructed that reveal previously unseen aspects of the basic mechanisms that determine the outcome of atomic collisions. Details of atomic and molecular structural features can be explored by numerical experiments. Elaborate computer codes have been constructed that provide the data on atomic and molecular processes needed for the interpretation and prediction of the behavior of laboratory, fusion, terrestrial, and astrophysical plasmas.

Atomic physics is but a subclass of an even broader area of research, now canonized as a Division of the APS under the rubric Atomic, Molecular, and Optical ("AMO") physics. In this section we have chosen some representative examples of the scope of atomic physics in several areas. Many other important aspects of AMO physics are contained in other articles in this volume: molecular astrophysics—Herschbach; Bose-Einstein condensation and control of atoms by light—Wieman *et al.*; quantum optics and precision spectroscopy—Hänsch and Walther; the laser—Lamb *et al.* A short history of atomic, molecular, and optical physics is contained in the article by Kleppner.

II. COLD COLLISIONS

T. F. Gallagher

Recent developments in the control of atoms by light (see Wieman *et al.*, this issue) have led to the extension of atomic collision studies to the domain of ultracold atoms. Alkali atoms in a magneto-optical trap (MOT) typically have temperatures of hundreds of microdegrees Kelvin, and as a result collisions between them are qualitatively different from collisions between room-temperature or more energetic atoms. The collisions last for a long time, tens of nanoseconds rather than picoseconds. This time is longer than the radiative lifetime of the excited alkali atoms, so it is likely that excited atoms decay in mid collision, and it is possible to influence these collisions to some extent with near-resonant laser light. The collisions velocities are so low that the de Broglie wavelength λ_B is larger than the typical interaction length. Equivalently, the scattering is mainly *s*-wave scattering, and whether the interatomic interaction is attractive or repulsive determines the conditions under which a Bose-Einstein condensate can be created (see below).

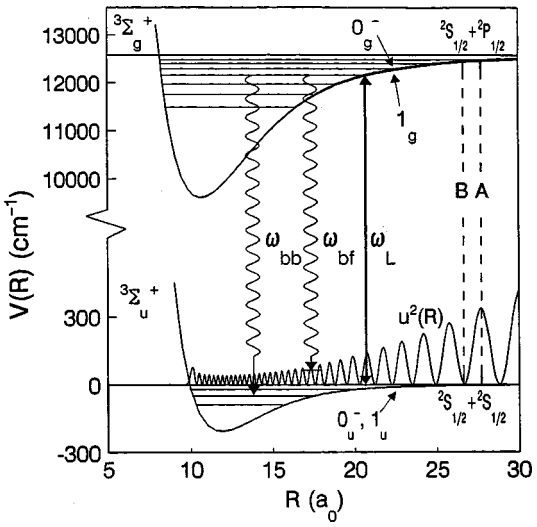

FIG. 1. Cold atomic photoassociation. Colliding atoms incident on the ground-state potential are excited by a laser of frequency ω_L to bound excited states. At low temperature, the photon absorption rate exhibits a highly resolved peak when ω_L is tuned across a free-bound transition. The triplet states of Rb_2 are shown in this example. The solid oscillating curve shows the square of an approximate radial wave function $u(R)$ of the colliding atoms. From Miller, Cline, and Henzen (1993).

Traditionally, one of the most useful ways of studying atomic collisions has been collisional line broadening (Gallagher, 1996). For cold collisions one form line broadening takes is photoassociation spectroscopy (Thorsheim *et al.*, 1987). The essential notions of photoionization spectroscopy for Rb are shown in Fig. 1 (Heinzen, 1996). This shows the interatomic potential curves for two Rb atoms when both are in the ground state and when one is in ground and the other in the excited state. Only the attractive potential curve from the excited state is shown. (There is also a potential that is repulsive at long range, but we ignore it for the moment). In a MOT trap most atoms exist in the $s+s$ dissociation continuum, connected to two *s* states as the interatomic spacing $R\rightarrow\infty$. The atoms have low translational energy, <1 mK, and the squared amplitude of the wave function for the relative motion of two such ground-state atoms at relatively small separations is shown in Fig. 1. This pair of atoms can absorb a photon tuned to the red of the Rb $5s_{1/2}$-$5p_{1/2}$ atomic transition, making a transition to the more deeply bound molecular excited state. It is more deeply bound at long range due to the resonant

[2]The best sourcebooks for an overview of activities in atomic collision are the proceedings of the biennial International Conference on the Physics of Electronic and Atomic Collisions (ICPEAC). See, for example, J. B. A. Mitchell *et al.*, Eds, 1996 ICPEAC XIX (American Institute of Physics, New York).

dipole-dipole coupling of the molecular states $5s_{1/2}+5p_{1/2}$ and $5p_{1/2}+5s_{1/2}$, which are degenerate at infinite internuclear separation.

The temperature of the atoms in a MOT is less than 300 μK, which corresponds to 6 MHz. Therefore, instead of a continuous far wing of the resonance line, like that observed in a higher-temperature gas, well resolved transitions to high vibrational levels of the excited state are observed. The excited molecules can decay to bound vibrational levels of the ground state by path ω_{bb} of Fig. 1 or, more often, to the dissociative continuum states, by path ω_{bf} with enough kinetic energy for the atoms to escape from the trap. The loss of atoms from the trap is the usual method of detecting that a free-bound transition has been driven in the first place. Some of the atoms do decay to high vibrational levels of the ground state, forming translationally cold molecules, as has been observed by photoionizing the dimers and detecting the dimer ions using a time-of-flight technique.

Photoassociation spectroscopy gives direct insight into the scattering of the cold atoms. Since λ_B is roughly $400\,a_0$, it is far greater than the range of the interatomic potential between two ground-state atoms, as shown by Fig. 1, and their scattering is thus dominated by *s*-wave scattering. On a longer length scale than the interatomic separations shown in Fig. 1 we can represent the interatomic motion by a wave function that has a sinusoidal dependence on R, the interatomic distance. If there is no interaction between the two atoms the sine wave has a zero at $R=0$. If the interaction is attractive the nodes of the wave function are pulled towards $R=0$, and if the interaction is repulsive the nodes are pushed away from $R=0$. These phase shifts of the wave function are often described by the scattering length a, which is proportional to the tangent of the phase shift. If the interaction is attractive, $a<0$, while it is repulsive if $a>0$.

The scattering length for two ground-state atoms can be extracted from the photoassociation spectrum using the Franck-Condon principle. Briefly, each antinode of the ground-state vibrational wave function leads to strong transitions to vibrational states with their outer turning points at the same R. Thus the transitions near the dashed line labeled A in Fig. 1 are strong. On the other hand, transitions at a slightly longer wavelength, resonant with transitions near the dashed line labeled B, are vanishingly weak since there is a node in the ground-state wave function at this interatomic spacing. In other words there is a slow modulation in the intensity of the lines in the photoassociation spectrum, which can be used to generate the wave function of the ground vibrational state and determine its phase shift relative to a sine wave starting from $R=0$. Measuring the phase shift, or equivalently, the scattering length tells whether or not it is possible to make a Bose-Einstein condensate in the system. It is possible if $a>0$, but if $a<0$ the atoms attract each other and BEC becomes more difficult, although it in fact has been achieved for Li, where $a<0$.

The collisions of cold atoms have shown initially surprising phenomena, and it has been possible to control them in a way not usually possible. It is likely that there will be many interesting future developments as well. One example is the use of cold atoms to make cold molecules. The first reports of the production of cold Cs_2 molecules came from Fioretti *et al.* (1998), and already a number of other cold-molecule experiments have been successful.

III. ACCELERATOR-BASED ATOMIC COLLISIONS

Sheldon Datz

Accelerator-based atomic physics covers a huge number of phenomena ranging from multiple ionization events and electron capture from pair production, in very violent collisions, to charge transfer and electron-ion recombination in rather more delicate ones.[3] The increasing availability of high-energy accelerators and the development of sources that produce multicharged ions with large stored energy, coupled with greater sophistication in experimental techniques, has brought about a considerable increase in our understanding of these processes in recent years. Some examples of specific areas of recent accelerator-based atomic physics research are given below.

A. Cold-target recoil-ion momentum spectroscopy

An excellent example of experimental refinement is the cold-target recoil-ion momentum spectroscopy method for analysis of collision phenomena (Ulrich *et al.*, 1998). The technique employs a well-defined target in the form of a precooled supersonic gas jet that crosses the projectile beam. Collision products are extracted by an appropriate electric field and detected by position-sensitive detectors. The position and time-of-flight information are used to calculate the momentum of the collision products with high precision. This technique makes it possible to determine the full momentum vectors of all collision products yielding a kinematically complete experiment. It has been employed in the last ten years in a wide range of experiments including collisions of ions, electrons, photons, and exotic projectiles with atoms, molecules, and clusters. The technique yields detailed information about the collision, including the determination of impact parameter, scattering plane, energy loss, and scattering angles. In addition, it allows full detection at all solid angles of the emitted electrons. In two-body systems, as in the case of electron transfer, the momentum balance between projectile and target allows for a measurment of the energy gain, which is sufficiently precise to determine individual levels for transfer into a given n state.

[3]See, for example, *Atomic Physics; Accelerators* (Marton and Richard, 1980).

B. Ultrarelativistic ion energies

Atomic collisions at ultrarelativistic energies (6.4-TeV S ions and 33.2-TeV Pb ions) have been studied using the SPS synchrotron at CERN (Vane *et al.*, 1997). At these energies, the electric fields have Fourier components representing energies greater than twice the rest mass, $h\nu > 2m_0c^2$, and electrons can be promoted from the negative continuum to produce electron-positron pairs (via two virtual photons) or, alternatively, to promote an electron to a bound state of the projectile, thereby changing its charge. This process, dubbed capture from pair production, can be responsible for beam loss in relativistic colliders, for example.

C. Electron-ion recombination

At the other end of the energy scale, highly accelerated ions may be used to study collisions at very low center-of-mass energies ($\gtrsim 1$ meV), using ''merging beams.'' An atomic ion can capture an electron and be stabilized by the emission of a photon (radiative recombination). In dielectronic recombination, the dominant process at high temperatures, an electron from the continuum can be captured into a bound state by the simultaneous excitation of a previously bound electron (inverse Auger effect) and the doubly excited state can be stabilized by the emission of a photon,

$$A^{q+}(n,\ell) + e \rightarrow A^{(q-1)+}(n'\ell', n''\ell'') \rightarrow A^{(q-1)+}(n\ell, n'\ell') + h\nu. \quad (1)$$

This is a resonant process that requires a specific collision energy to form a given doubly excited state.

At Oak Ridge National Laboratory, a tandem Van de Graaff accelerator was used to create an energetic multiply-charged ion beam which was merged with a collinear electron beam and the resultant reduced charge from the dielectronic recombination ion measured (Datz and Dittner, 1988). Why use an accelerator? High-charge states are easily obtained. The accelerated beams have a lower electron-capture cross section from background gas, and the higher-energy electron beams needed to achieve comparable velocities have higher space-charge limited currents. The system was used to measure $\Delta n = 1$ dielectronic recombination cross sections for a variety of ions from B^+ to S^{6+}. The resolution of ~ 4 eV was sufficient for integral measurements only. Much higher resolution was later achieved at Aarhus using a much improved merged electron beam ring. The advent of ion storage rings initiated a qualitative improvement in the study of electron-ion collisions (Larsson, 1995). A storage ring comprises a closed magnetic loop for the circulation of ions that have been injected from an ion source. Such ion storage rings are presently in operation in Sweden, Denmark Germany and Japan. The ions may be accelerated in the ring up to the limit of magnetic containment. In the case of the CRYRING in Stockholm, the strength is 1.44 Tm, equivalent to 96 MeV times the ion charge divided by the mass. During its storage time, the ion can relax from metastable states created in the source and, in the case of molecular ions, vibrotational levels can also decay. In one of the straight sections of the ring, an electron beam is merged with the ion beam over a length of 1 m. The original purpose of this merged beam was to reduce the momentum spread in the stored ion beam (''cooling''). This is done by matching the ion and electron beam velocities and taking up the random motion within the ion beam by Coulomb scattering from ''cold'' electrons. The longitudinal energy spread of the electron beam is negligible and the transverse spread has now been reduced to 1 meV.

An intentional mismatch of velocities creates a variable-energy ion-electron collision target. The results obtained include highly precise dielectronic resonances which have led to more accurate determinations of the structure of doubly excited states. An unusual and, at this time, unexplained finding is a large increase in radiative recombination cross section above theory at very low collision energies.

In similar experiments, molecular ions can recombine and, upon regaining the ionization energy, dissociate into neutral fragments. Precision measurements of dissociative recombination of molecular ions in the energy range of 1 meV to 50 eV have been made. For diatomic molecular ions, the final states of the neutral atoms formed have been measured using ring techniques. The resonant structures and the fractionations observed present a challenge to current theory.

IV. FUNDAMENTAL MEASUREMENTS IN ATOMIC COLLISION PHYSICS

Hans Kleinpoppen

A. Introductory remarks

Atomic collision physics can be broadly divided into cross-section measurements and analyses of fundamental quantum-mechanical processes. Such processes, particularly with regard to atomic and electron spin correlations and resonances, have only been accessible to detailed investigation since the second half of this century. Studies of this kind are particularly connected with ''complete atomic scattering experiments'' (see Sec. IV.B).

Approximately a hundred years ago the area of atomic collision physics was opened up when photoionization was discovered by H. Hertz in 1887 and electron collision cross sections were estimated by P. Lenard in 1903 from processes in Braun's classical electron tube. Lenard postulated that the electron impact cross section appeared to be much smaller than the atomic cross sections already known from chemical processes and kinetic theory. However, Lenard's experiments failed to reveal the presence of the massive positively charged nucleus of atoms discovered by E. Rutherford in 1911. While the detection of the inelastic energy loss of elec-

trons in electron-impact excitation of atoms was discovered by J. Franck and G. Hertz in 1913, electron scattering from rare-gas atoms carried out by Ramsauer, Ramsauer and Kollath, and Townsend and Bailey in the 1920s revealed specific minima in the total electron-atom cross sections. In 1931 Bullard and Massey detected structure in the differential cross section which could theoretically be interpreted as interference effects in the partial waves of different orbital momenta. Early calculations by N. F. Mott (1929) predicted electron spin polarization through spin-orbit interaction in electron scattering by heavy atoms; however, this sensational prediction by Mott, in the 1920s, was only observed, much later, by Shull, Chase, and Myers (1943). A series of measurements to produce intense beams of polarized electrons and to apply collisions of them with polarized or unpolarized atoms only took place in the second half of this century. Since that time, further highlights in atomic collision physics were the scattering of electrons by polarized atoms and coincidence experiments between atomic particles and photons. Cross-section measurements were continuously stimulated by quantum-mechanical theories of atomic collisions by Born, Mott, Oppenheimer, Massey, and others [see, for example, Mott and Massey (1965) and more modern versions of theories by Bransden (1983), Joachain (1983), and Burke and Joachain (1995)]. One of the outstanding cross-section measurements in atomic collisions was connected with electron scattering on atomic hydrogen. The primary scientific aspect of such experiments was that they represented the simplest and most fundamental quantum-mechanical collision phenomenon in comparison to more complicated many-electron atoms. Experimentally, the production of atomic hydrogen targets was a very demanding and difficult problem, and, to a certain degree, it still remains a problem today. A pioneering experimental step forward in producing a sufficiently intense atomic hydrogen target was pioneered by Fite and Brackman (1958).

Another important electron impact excitation problem was related to the polarization of resonance radiation from atoms excited by electrons at or close to the threshold energy of the exciting process. There were old discrepancies between the theories of Oppenheimer (1927, 1929) and Penney (1932) and the experiments of Skinner and Appleyard (1927) which were only resolved much later by studying fine and hyperfine structure effects of threshold polarization in both theory and experiment. The fundamental quantum-mechanical theory of impact polarization, introduced by Percival and Seaton (1958), correctly took account of the fine and hyperfine splittings and the level widths of the excited states from which polarized radiation from the alkali resonance lines could be measured (Hafner *et al.*, 1965). Such polarizations of impact line radiation can now be based on a proper theoretical quantum-mechanical theory, and numerous experimental comparisons are available confirming the theory of Percival and Seaton.

Cross-section measurements have been carried out since, approximately, the beginning of this century and they are important tests of atomic collision theories. In addition they are relevant to applications in plasma physics, astrophysics, and atmospheric physics; for examples, see reference books such as *Electronic and Ionic Impact Phenomena*, Vol. 1–4, by H. S. W. Massey (1979); *Atomic Collisions*, by E. W. McDaniel (1989); *Atomic and Electron Physics–Atomic Interactions*, by B. Bederson and W. L. Fite (1968), as well as the biennial series of proceedings of ICPEAC (footnote 2).

B. Complete atomic scattering experiments

1. Correlation and coincidence experiments

I shall now highlight developments (personally selected) that can be linked to correlation and coincidence measurements between atomic particles (including spin correlations) and to the so-called ''complete (or perfect)'' atomic scattering and photoionization experiments. Initial proposals for such types of experiments can be traced to the pioneering papers of U. Fano (1957) and B. Bederson (1969, 1970). The idea of ''complete'' experiments refers to the requirement that initially the collision process be described by a quantum-mechanical pure state vector. This means, for example, that particles A and B may be in quantum states $|n_A J_A m_A\rangle$ and $|n_B J_B m_B\rangle$ with the corresponding quantum numbers n, J, and m for the two particles. The interaction process of the collision with the particles in pure quantum states can, at least in principle, be described by a quantum-mechanical Hamilton operator $H_{\rm int}$, which is determined by the interaction potential between the colliding partners. As a consequence of the linearity of the Schrödinger equation, the total system of the particles after the collision will also be in pure quantum states. In other words, we can represent atomic collision processes between atomic particles in pure quantum states as follows:

$$|\varphi_{\rm in}\rangle = |A\rangle|B\rangle \xrightarrow[\text{linear operator}H_{\rm int}]{} |\varphi_{\rm out}\rangle = |C\rangle|D\rangle\cdots|K\rangle\cdots . \tag{2}$$

Before the collision, the colliding particles are in the joint quantum state $|\varphi_{\rm in}\rangle$; after the collision the ''collisional products'' are in the state $|\varphi_{\rm out}\rangle$.

If the state vector $|\varphi_{\rm out}\rangle$ after the collision has been extracted from an appropriate experiment, it may be described by applying the quantum-mechanical superposition principle in the form

$$|\varphi_{\rm out}\rangle = \sum_m f_m \varphi_m , \tag{3}$$

where φ_m are wave functions of possible substates of the state vector $|\varphi_{\rm out}\rangle$ and f_m are complex amplitudes associated with the collision process. The extraction of the state vector $|\varphi_{\rm out}\rangle$ represents the *maximum information and knowledge* that can be extracted from the experimental analysis of the collision process. Experiments that are successful in providing such maximum information are known as *complete experiments*. (Bederson ini-

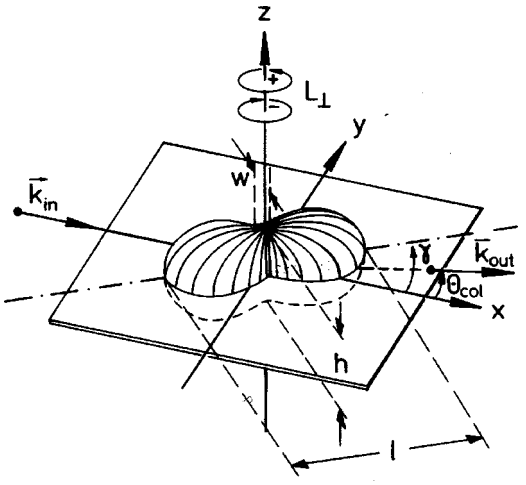

FIG. 2. Schematic illustration of an electron charge cloud for a coherently excited P state induced by an incoming particle parallel to the x direction [after Andersen *et al.* (1984)].

tially used the expression "perfect experiments," but they are generally now called "complete experiments.")

Complete experiments on atomic collision processes require a high degree of experimental effort and special methods, which have only been successfully applied since the beginning of the 1970s. We cannot refer to primary citations because of space limitations; many review articles and books should serve instead, for example, those of Andersen *et al.* (1988, 1997).

Macek and Jaecks (1971) first developed a concise theory of the angular and polarization correlation between inelastically scattered electrons and polarized photons from excitation/deexcitation processes of atoms. With regard to the relatively simple singlet excitation process of $^1P_1$ states of helium, i.e.,

$$e(E)+\mathrm{He}(1^1S_0)\rightarrow \mathrm{He}(n^1P_1)+e(E-E_{\mathrm{thr}}) \rightarrow \mathrm{He}(1^1S_0)+e(E-E_{\mathrm{thr}})+h\nu, \quad (4)$$

two amplitudes describing coincidence signals between the inelastically scattered electron and the photon from the excitation process can be extracted from the coincidence experiment, namely, f_0 for the magnetic sublevel $m_1=0$ and f_1 for the sublevels $m_1=\pm 1$ of the $^1P_1$ state. The helium excitation/deexcitation $1^1S_0\rightarrow 3^1P_1\rightarrow 2^1S_0$ was investigated by observing the photon emitted from the 3^1P_1 state in coincidence with the inelastically scattered electron in the forward scattering direction; by measuring the photon linear polarization with reference to the incoming electrons, experimenters could confirm the selection rule $\Delta m=0$ for the magnetic quantum number according to the Percival-Seaton (1958) theory of impact polarization of line radiation. They also could correct the previous discrepancy with theory of the noncoincidence threshold polarization measurements. Eminyan *et al.* (1973, 1974) extended the coincidence experiment by measuring a more general electron-photon angular correlation in the scattering place and determined a set of inelastic excitation amplitudes of the 2^1P_1 state of helium for the first time. Standage and Kleinpoppen (1976) measured a full set of Stokes parameters (Born and Wolf, 1970) of the photon from the $3^1P_1\rightarrow 2^1S_0$ excitation in coincidence with the scattered electron and obtained a complete amplitude analysis as well as the orientation vector $L_\perp$ (i.e., a finite expectation value of the angular momentum in the 3^1P_1 state) and an alignment (i.e., a nonisotropic distribution of the magnetic sublevels JM with expectation values $\langle M\rangle = \langle J^2\rangle/3$ of the excited $^1P_1$ state in accordance with the analysis of Fano and Macek, 1973). In addition to the amplitude and orientation/alignment analysis the "charge cloud" of the excited $^1P_1$ state of helium can also be determined (Andersen *et al.*, 1984).

Figure 2 shows an example of a collisionally induced electron charge cloud distribution of a $^1P_1$ state detected by the coincidence of the scattered electron in the k_{out} direction and the photon detected in the z direction. The scattering plane is defined by the directions of the incoming k_{in} and the outgoing k_{out} relative momentum vectors of the electron. The atomic charge can be characterized by its relative length (l), width (w), and height (h), its alignment angle (γ) and its angular momentum ($L_\perp$).

Following the definitions of Born and Wolf (1970), the Stirling group (Standage and Kleinpoppen, 1976) could also prove that photon radiation from the electron impact excited He(3^1P_1) state is completely polarized and the relevant degree of coherence for its excitation is approaching 100%. Many electron-photon coincidence experiments have been reported since the middle of the seventies [see, for example, Andersen *et al.* (1988)] and their results on coherence and correlation effects have opened up completely new research topics in atomic collision physics.

As already mentioned, electron impact excitation of atomic hydrogen is both one of the most fundamental and one of the simplest atomic collision processes. However, even for the excitation of the Lyman-α radiation, i.e., the $2^2P_{1/2,3/2}$ state decaying into $1^2S_{1/2}$ state, by electron impact there was a long-standing discrepancy between the theory and the experimental electron Lyman-α photon coincidences which has only recently been resolved (Yalim *et al.*, 1997).

Many measurements on collisions between heavy atomic particles (neutral or ionized atoms) and atoms have been reported since the middle of the 1970s, for example, photon-particle (neutral or ionized atoms) coincidence experiments, in connection with charge-exchange excitation of helium and molecular hydrogen with He^+ ions as projectiles. Angular correlation measurements from direct excitation of helium atoms have also been performed. Out of the many measurements of heavy-particle–photon excitation [see the review by Andersen *et al.* (1997)], we describe the alignment of the $2P$ state of atomic hydrogen produced in collisions between protons and atomic hydrogen as reported by the Hippler and Lutz group (Hippler *et al.*, 1988).

The collision process considered is described by the following reaction with two outgoing results:

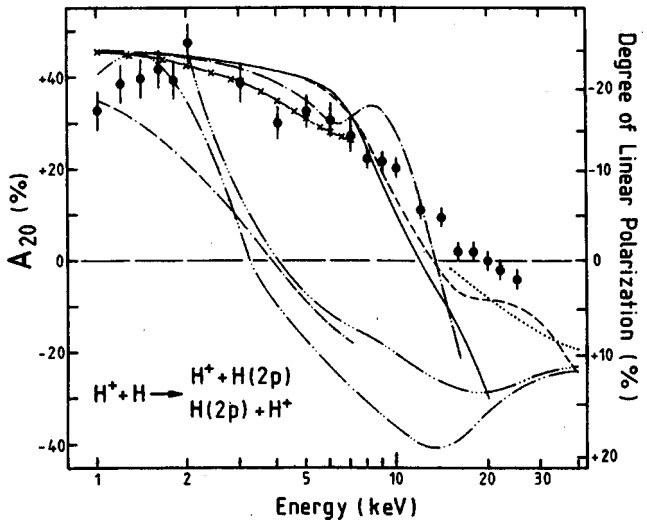

FIG. 3. Integral alignment A^{20} (left-hand scale) and linear polarization (right-hand scale) of the Lyman-α radiation for $H(2P)$ production of $H^+ + H$ collisions vs incident energy of the protons. Experimental data by Hippler *et al.* (1988) are compared to various calculations. Best agreement is obtained with calculations that include quasimolecular rotational coupling.

$$H^+ + H \begin{cases} \nearrow H^+ + H(2P) \\ \searrow H(2P) + H^+ \end{cases} \tag{5}$$

i.e., a proton beam crosses an atomic hydrogen beam. At incident energies of a few keV the $H(2P)$ production results from a united-atom $(2p\sigma\text{-}2p\pi)$ rotational coupling. Lyman-α photons from the decay of the $H(2P)$ state were detected perpendicular to the primary proton beam direction with a polarization-sensitive device. The degree of linear polarization $p = I_\parallel - I_\perp / I_\parallel + I_\perp$ of the Lyman-α radiation is defined with the light intensity components polarized parallel and perpendicular to the proton beam direction.

The polarization p can be related to the integral alignment A_{20} of the $H(2P)$ state by the following relations:

$$A_{20} = \frac{Q_1 - Q_0}{Q(2P)} = \frac{6p}{p-3}, \tag{6}$$

with the total excitation cross section $Q_1 (= Q_{-1})$ and Q_0 for the magnetic sublevels m_1, m_0 and $Q(2P) = Q_0 + 2Q_1$ as the total cross section for the $2P$ state.

Figure 3 shows experimental data for the integral alignment A_{20} in comparison to several theoretical predictions. The theories fall into two categories in which either only atomic wave functions are used or, alternatively, molecular states or combinations of both atomic and molecular states are employed. Only theories within the second category include a quasimolecular rotational coupling mechanism. Good agreement between experiment and theory is obtained with the molecular orbital calculations. Such experiments are considered as a very important test case for theories of heavy-particle–atomic collisions.

2. Electron scattering by atoms in laser fields

Electron scattering by atoms in laser fields of various intensities has become of fundamental importance in understanding the interactions of the colliding electron and the electromagnetic field of the photon. Several outstanding contributions are listed here:

(a) Transfer of energy in multiples of the photon energy $h\nu$ to and from electrons while they are undergoing elastic scattering by atoms is described by the process

$$e(E) + A + nh\nu \rightarrow e(E \pm mh\nu) + A. \tag{7}$$

Such a process was first observed by Weingartshofer *et al.* (1977).

(b) The energy balance in electron impact excitation of atoms can be made up jointly by the electron energy E_0 and the photon energy in a photon and electron impact process such as $h\nu + e(E_0) + A \rightarrow A^* + e(E_0 + h\nu - E_{\text{thr}})$.

(c) As a mirror symmetric inverse process of the above electron-photon coincidences from electron impact excitation of atoms (reported in Sec. B.1) Hertel and Stoll (1974) studied electron scattering in conjunction with the resonance absorption of a laser photon energy of $h\nu = E_{\text{thr}} - E$ with E as the ground-state energy and E_{thr} as the threshold energy for the excited state. The analysis of the angular distribution related to the photon laser polarization again allows a description of the scattering process in terms of two amplitudes and their phase difference for $S \rightarrow P \rightarrow S$ transitions.

(d) By inducing a resonance absorption of atoms by photons, one can populate an excited state A_1^*. Electron-photon coincidences can then be detected from an even higher excited state A_2^*, i.e., $h\nu + e(E) + A \rightarrow A_1^* + e(E) \rightarrow A_2^* + h\nu_1 + e(E - E_{\text{thr}})$. Excitation amplitudes have been extracted from such "stepwise excitation electron-photon coincidences" for electron mercury scattering.

3. $(e,2e)$ ionization processes of atoms

With regard to ionization of atoms by electrons, studies of the coincidence between the impinging scattered electron and the electron released from the ionization process, $(e,2e)$ experiments, were first reported by Amaldi *et al.* (1969) and by Ehrhardt *et al.* (1969). Since that time, many $(e,2e)$ and even $(e,3e)$ processes have been investigated, including theoretical approximations. As with the electron-photon coincidence experiments these represent more sensitive tests of a theory than the traditional total-cross-section measurements of ionization. As an example, we discuss here data on electron impact ionization of atomic hydrogen and refer the reader to other examples, e.g., to the review by McCarthy and Weigold (1991) and the monograph by Whelan and Walters (1997).

We first introduce the definition of the triply differential cross section: $d^3Q\ (E_0, E_a, E_b, \theta_a, \theta_b, \varphi_b) / dE_b d\Omega_a d\Omega_b$ with the polar scattering angles θ_a and θ_b for the two electrons detected with an azimuthal angle $\varphi_b = 0$ (defining the scattering plane); θ_a and θ_b are fi-

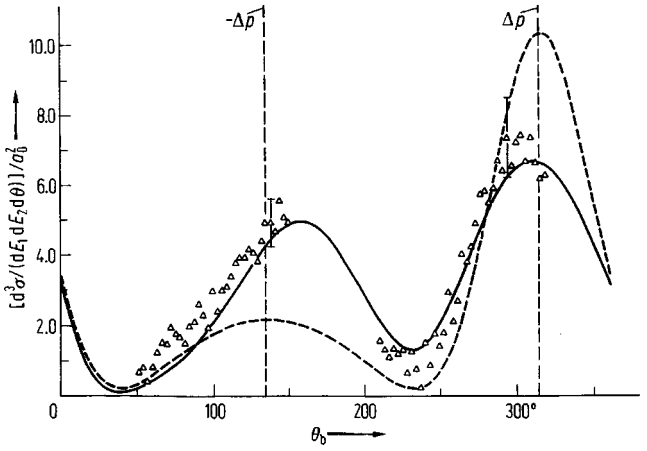

FIG. 4. Triple differential cross section for the $(e,2e)$ angular correlation of atomic hydrogen as a function of the scattering angle θ_b with fixed $\theta_a=4°$, $E_b=5$ eV and the primary incident electron energy $E_0=150$ eV [after Klar *et al.* (1987)]: dashed curve, Born approximation; solid curve, Coulomb-correlation method after Jetzke *et al.* (1989). The angle on the abscissa for θ_b is measured from the direction of the incident electron. The dotted vertical lines show the angle for scattering parallel ($\Delta\mathbf{p}$) and antiparallel ($-\Delta\mathbf{p}$) to the vector of momentum transfer $\Delta\mathbf{p}=\lambda\Delta\mathbf{k}$.

nite, the energy of the scattered electron is E_a and the energy of the incoming electron is E_0 (E_b is then calculable from the energy balance); $d\Omega_a$ and $d\Omega_b$ are the solid angles for the coincident detection of the two electrons.

Figure 4 gives one example of theoretical and experimental data on $(e,2e)$ processes for electron impact ionization of atomic hydrogen. As can be seen, the Born approximation essentially fails to reproduce the experimental data while the Coulomb correlation method appears to be in reasonable agreement. Direct coincidence measurements of electron momentum distributions of the ground state of atomic hydrogen and other atoms have also been performed.

4. Polarized-electron/polarized-photon interactions with atoms

This is the subfield where most of the exciting new approaches in experimental atomic collision physics are found at present, combining coincidence measurements with electron and atomic spin analysis. Early pioneering papers include the electron-polarized atom recoil experiment of Rubin *et al.* (1969) and the Mott spin polarization measurements of unpolarized electron scattered by partially polarized potassium atoms (Hils *et al.*, 1972). Bederson, Rubin and collaborators applied a Stern-Gerlach hexapole magnet as a velocity selector and a polarizer to polarize potassium atoms. The electron impact process may result in a change of the polarization of the initially polarized atoms, which depend on Coulomb direct interaction (amplitudes f_0 and f_1 for the magnetic sublevels $m=0$ and $m=\pm1$) and Coulomb exchange interaction (amplitudes g_0 and g_1). An E-H gradient analyzer acts as a "spin filter," which can be adjusted to pass only those atoms from the collision area to the detector which have changed their spin state into the antiparallel direction compared to the spin direction of the atoms leaving the Stern-Gerlach magnet.

This experiment (undertaken approximately 30 years ago) could only be matched, some years later, by the JILA experimentalists S. J. Smith and collaborators (Hils *et al.*, 1972), who introduced an alternative experiment in which a potassium atomic beam was polarized (and focused) by a commercial Hewlett-Packard magnetic hexapole and the spin polarization by the elastically scattered electrons was measured by a Mott detector. Neglecting spin-orbit interactions, they could then describe electron scattering by one-electron-atoms by the spin reactions shown in Table I, in which $e(\uparrow)$, $e(\downarrow)$, $A(\uparrow)$, and $A(\downarrow)$ are completely spin-polarized electrons or atoms and only Coulomb direct and Coulomb exchange interactions take part.

On the other hand, only partially polarized electrons and atoms (one-electron atoms) are so far available experimentally (i.e., spin-polarized electrons and spin-polarized atoms with their polarization degree P_e, P'_e, P_a, and P'_a before and after scattering), which implies that combined measurements of spin reactions should be possible to determine both the modules of the amplitudes f and g and their relative phase difference. For example, the above experiment of Hils *et al.* (1972) gives information on the ratio $|f|^2/\sigma(E,\theta)=(1-P'_eP_a)$, that is, the Coulomb direct cross section divided by the full differential cross section, which is determined by knowing the degree of polarization of the atomic target (P_a) and measuring the spin polarization (P'_e), of the scattered electrons.

The next step in polarized-electron/polarized-atom collisions was the detection of ion symmetries. The ion asymmetry in electron impact ionization can be seen in

TABLE I. Electron scattering by one-electron atoms.

Scattering process	Interactions	Amplitudes	Cross sections
$e(\uparrow)+A(\downarrow)\rightarrow A(\downarrow)+e(\uparrow)$	Coulomb direct	f	$\lvert f\rvert^2$
$\rightarrow A(\uparrow)+e(\downarrow)$,	Coulomb exchange	g	$\lvert g\rvert^2$
$e(\uparrow)+A(\uparrow)\rightarrow A(\uparrow)+e(\uparrow)$,	Interference between direct and exchange interaction	$f-g$	$\lvert f-g\rvert^2$
Full differential cross section: $\sigma(E,\theta)=1/2\{\lvert f\rvert^2+\lvert g\rvert^2+\lvert f-g\rvert^2\}$			

experiments in which polarized electrons collide with polarized atoms and ions are produced; by introducing the notations $N^{\uparrow\uparrow}(I)$ and $N^{\uparrow\downarrow}(I)$ for the number of ions produced, with the relevant spins of the incoming electrons and the target atoms either parallel or antiparallel to each other one can define the so-called ion asymmetry by the expression

$$A_{\text{ion}}=\frac{N^{\uparrow\uparrow}(I)-N^{\uparrow\downarrow}(I)}{N^{\uparrow\uparrow}(I)+N^{\uparrow\downarrow}(I)}. \tag{8}$$

The first experiments of this type were carried out with polarized atomic hydrogen (Alguard *et al.*, 1977) and with polarized sodium atoms (Hils and Kleinpoppen, 1978).

In electron scattering by heavy atoms such as rubidium and cesium, spin-orbit interaction between the projectile electron and the target atom must be taken into account in addition to the direct Coulomb and exchange interactions. This situation is similar to that for the normal fine structure of excited atoms or the photoionization of heavy alkali atoms, in which spin-orbit interactions increase with increasing mass of the atoms involved. Six amplitudes are necessary for the description of elastic electron scattering on heavy alkali atoms, which means that 11 independent quantities, i.e., six moduli and five phase differences, have to be determined for complete analysis of the scattering process. A start in determining the six amplitudes has already been made with spin-polarized electrons scattered elastically by spin-polarized cesium atoms in the ground state (Brum *et al.*, 1997). By their measurements spin asymmetries could be detected including the one predicted by Farago (1974, 1976) as an interference effect between the spin-orbit interaction and the spin-exchange interaction.

The complication due to the large number of amplitudes is reduced by using target atoms without a resulting total electron spin (''spinless'' atoms), as for example with rare-gas atoms or two-electron atoms with opposite spins. Two spin reactions can be defined for the scattering of polarized electrons on spinless atoms A:

$$\begin{aligned}&(1)\ \ e(\uparrow)+A\rightarrow A+e(\uparrow), \quad h, \quad |h|^2,\\ &(2)\ \ e(\uparrow)+A\rightarrow A+e(\downarrow), \quad k, \quad |k|^2.\end{aligned} \tag{9}$$

We denote the first process, as before, as a direct process with amplitude h and the second one as a spin-flip process with amplitude k. The direct process can be superposed coherently with an electron exchange process; these processes cannot be individually observed due to their indistinguishability in the experiment. The spin polarization of the electrons after scattering determines the moduli $|h|$ and $|k|$ and their phase differences $\Delta\varphi=\gamma_1-\gamma_2$.

Figure 5 shows an example for the moduli of the above amplitudes and their phase differences from elastic electron-xenon scattering. As one can see, the modulus $|h|$ of the direct scattering amplitude shows a distinctive diffraction structure, which is due to the superposition of several partial waves of scattered electrons with various angular momenta. This structure is determined by the dipole and exchange interactions, as previously described in connection with the Ramsauer-Townsend effect. The modulus of the spin-flip amplitude $|k|$, which originates from the spin-orbit interaction is considerably smaller than that of the direct amplitude $|h|$; the spin-flip amplitude is primarily determined by the ($\ell=1$) partial wave of the scattered electrons, which has the result that the diffraction structure is hardly discernible.

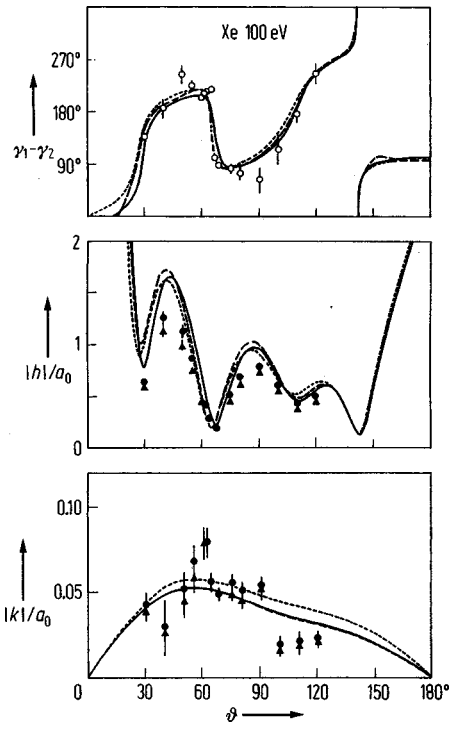

FIG. 5. Moduli of amplitudes $|h|$ and $|k|$ and phase differences $\gamma_1-\gamma_2$ between the two amplitudes for elastic scattering of polarized electrons on xenon atoms, as a function of the scattering angle at an energy of 100 eV. Experimental data points with error bars after Berger and Kessler (1986). The dotted lines and solid curves represent various theoretical predictions: after Haberland *et al.* (1986), McEachran and Stauffer (1986), Awe *et al.* (1983). The data $|h|$ and $|k|$ are given in units of the Bohr radius a_0 and are normalized to the measured differential cross section $\sigma=|h|^2+|k|^2$.

Finally I should like to mention a new kind of complete experiment on photoionization of partially polarized atoms reported by Plotzke *et al.* (1996). By applying a hexapole magnet, they were able to polarize and focus atoms on the target area, where a small magnetic guiding field orients the atom spin or J-vector parallel or antiparallel to the direction of the incoming synchrotron radiation of BESSY (Berliner Elektronenspeicherring-Gesellschaft für Synchrotronstrahlung), which is linearly polarized. Photoionization experiments with randomly oriented targets yield two independent parameters, the cross section σ and the parameter β of the angular distribution of the emitted photoelectrons (Yang, 1948). However, this description of the photoionization process is restrictive and averages over the finer details. Klar

and Kleinpoppen (1982) have shown that ''complete'' information on the photoionization process can be obtained by analyzing the photoelectron angular distributions from partially polarized atoms. This method is complementary to the spin analysis of photoelectrons from unpolarized atoms (see, for example, Heinzmann and Cherepkov, 1996).

A new approach to complete photoionization experiments, by means of coincidence measurement between autoionized electrons and polarized fluorescent photons, in the region of the $3p$-$3d$ resonance in calcium has recently been reported.

C. Summary

Atomic collision physics has developed to a high degree of sophistication particularly due to advanced experimental technology combined with ever-increasing computational capability. Recent emphasis of ICPEAC[1] (Aumayr and Winter, 1998) has been on fundamental quantum-mechanical aspects such as coherence, correlation, alignment, orientation, polarization and, lately, collisions of Bose-Einstein condensates. Recent experimental investigations that apply polarized electrons in electron-electron $(e,2e)$ and in electron-photon $(e,e\gamma)$ coincidence experiments have been reviewed by Hanne (1996a 1996b).

Limited space does not permit discussion of the many other important recent accomplishments in fundamental atomic collision physics, for example, superelastic scattering by polarized excited atoms, synchrotron radiation experiments, spin asymmetries based on spin-orbit interactions in electron-atom and ion-atom collisions, resonances, and resonant interactions with radiation fields.

While we have concentrated here on fundamental types of experiments, it should be emphasized that many theoretical investigations were crucial for the interpretation of ''complete atomic collision experiments.'' See, for example, Karl Blum's book, *Density Matrix Theory and Applications*, in which the most relevant theoretical papers are discussed and listed. More basic treatments in connection with atomic and quantum collisions and scattering theories are covered by, for example, Massey, 1979; Bransden, 1983; Joachain, 1983; Merzbacher, 1998.

In a lecture given by Sir Harrie Massey approximately one year before his death he stated

> We now have the opportunity for gaining deeper understanding of (atomic) collision mechanisms through providing information about the shapes and circulations of atomic wave functions in collision processes. The (experimental) techniques required are very elaborate. Indeed it is probably true that experiments in this field (of coherence and correlation) are among the most complicated in atomic physics today. They are very important for deepening our understanding of atomic collisions and it is essential that their very complexity should not be allowed to obscure their importance (Massey, 1979).

V. HIGH-PRECISION ATOMIC THEORY: THE FEW-BODY PROBLEM

G. W. F. Drake

A. Introduction

This section focuses on the remarkable advances that have taken place over the past fifteen years in the theory of atomic systems more complicated than hydrogen—specifically helium and other three-body systems. Since the time of Newton, the classic three-body problem has defied the best attempts of mathematicians to find exact analytic solutions. In the modern context, solutions to the three-body Schrödinger equation are equally difficult to obtain. However, once found to sufficient accuracy, they form the basis for studying the relativistic and quantum electrodynamic effects that must be included in order to account for the results of high-precision spectroscopic measurements. It is of course the advances in laser spectroscopy that provide the necessary accuracy to allow new and meaningful tests of quantum electrodynamics in systems more complicated than hydrogen, and possibly to find new physical effects. There is no guarantee that a consideration of pairwise interactions among the particles alone is sufficient or that there are no specifically three-body effects.

B. The nonrelativistic Schrödinger equation

The helium problem played an important role in the early history of quantum mechanics (Hylleraas, 1963). As pointed out by Max Born, the old Bohr-Sommerfeld quantization scheme worked perfectly well for hydrogen, and so helium became a crucial test of Schrödinger's (1926a) wave mechanics. Were it not for the e^2/r_{12} Coulomb repulsion between the two electrons, the three-body Schrödinger equation for helium would be separable, and therefore exactly soluble in terms of products of hydrogenic wave functions. Since the full equation is not separable, approximation methods must be applied, as described in the following sections.

The earliest tests involved the central-field approximation of Hartree (1928) in which each electron is assumed to move in the spherically averaged field of the other. Results for helium, and especially rubidium, yielded reasonable agreement with experiment and markedly different results from the classical orbital model. Hartree's result for the ionization energy of helium was 24.85 eV, as compared with the experimental value 24.60 eV. However, Hartree's central-field model, and its extension by Fock (1930) to include electron exchange, can never recover the remaining correlation energy of about 1 eV (relative to the Hartree-Fock ionization energy of 23.7 eV).

The Hartree-Fock approximation can be thought of as the best possible wave function that can be written in a separable product form. This has a clear physical meaning rooted in the shell model of an atom; but the exact

wave function cannot be expressed in this form. The key innovation of Hylleraas in 1927 [with influences from Slater (1928), as well as Max Born, Eugene Wigner, and Hans Bethe] stems from the realization that the triangle formed by the nucleus and the two electrons of helium is determined by the three lengths r_1, r_2 and $\mathbf{r}_{12}=|\mathbf{r}_1-\mathbf{r}_2|$, where $\mathbf{r}_1$ and $\mathbf{r}_2$ are the position vectors of the two electrons relative to the nucleus. Since the orientation of the triangle in space is not important, the essential dynamics of the system is contained in just these three variables out of the total of six (or equivalently $s=r_1+r_2$, $t=r_1-r_2$, $u=r_{12}$). With this in mind Hylleraas constructed a trial variational wave function for the ground state of helium consisting of a sum of terms of the form

$$A_{i,j,k}s^i t^j u^k \exp\left(-\frac{1}{2}Ks\right), \tag{10}$$

where each term has different powers i,j,k, and the $A_{i,j,k}$ are linear variational coefficients determined by simultaneously diagonalizing the Hamiltonian and overlap integrals in this basis set of functions [see Drake (1998) for a review of variational methods]. Early numerical experiments by Hylleraas and others [see Bethe and Salpeter (1957), Sec. 32 for a review] showed that just a few terms involving powers of $u=r_{12}$ (especially the odd powers) were sufficient to recover nearly all the correlation energy.

Further calculations with basis sets of increasing size and sophistication, culminating with the work of Pekeris and co-workers in the 1960s (see Accad, Pekeris, and Schiff, 1971) showed that nonrelativistic energies accurate to a few parts in 10^9 could be obtained by this method, at least for the low-lying states of helium and He-like ions. However, these calculations also revealed two serious numerical problems. First, it is difficult to improve upon the accuracy of a few parts in 10^9 without using extremely large basis sets where roundoff error and numerical linear dependence become a problem. Second, as is typical of variational calculations, the accuracy is best for the lowest state of each symmetry, but rapidly deteriorates with increasing n.

1. Recent advances

Modern spectroscopic accuracies in the sub-MHz range require theoretical energies accurate to a few parts in 10^{12} to make meaningful comparisons with experiment. Over the past 15 years, both of the above limitations on accuracy have been resolved by "doubling" the basis set so that each combination of powers i,j,k is included twice with different exponential scale factors (Drake, 1993a, 1993b). A complete optimization with respect to all the nonlinear parameters leads to a natural partition of the basis set into two distinct distance scales—one appropriate to the long-range asymptotic behavior of the wave function, and one appropriate to the complex correlated motion near the nucleus. The greater flexibility in the available distance scales allows a much better physical description of the atomic wave function, especially for the higher-lying Rydberg states where two sets of distance scales are clearly important. However, the multiple distance scales also greatly improve the accuracy for the low-lying states.

For the classic example of the ground state of helium, the nonrelativistic energy is now known to be

$$E_{\rm NR}=-2.903\,724\,377\,034\,119\,598\,13(23), \tag{11}$$

obtained by extrapolation from a doubled basis set containing 2114 terms. The accuracy is about one part in 10^{19}. Other results approaching this accuracy have been obtained in recent years, using both Hylleraas and other basis sets (Bürgers *et al.*, 1995, Goldman, 1998). The calculation of Baker *et al.* (1990) is significant for its accuracy, given that only 476 terms were used. The significant point is that all of these methods are evidently converging to the same numerical value.[4]

The same Hylleraas-type methods can in principle be applied to atoms more complex than helium, but the size of the basis set required for a given degree of accuracy and the demands on computer resources grow extremely rapidly with the number of particles. That is why alternative methods of more limited accuracy have been developed, such as multiconfiguration Hartree-Fock, configuration-interaction, many-body perturbation theory, finite-element, diffusion Monte Carlo, and variational Monte Carlo techniques. These techniques can readily be extended to arbitrarily complex systems, but the accuracy seldom exceeds one part in 10^6 for the energy. Hylleraas-type results with accuracies comparable to helium have been obtained only for lithium and similar four-body systems (Yan and Drake, 1998).

2. Asymptotic expansions

Results of similar accuracy are now available for all the higher-lying $1snl^{1,3}L$ Rydberg states of helium up to $n=10$ and $L=7$. One might object that these long strings of figures are just numerology with little physical content. However, with increasing L, one can give a full physical account of the variational results by means of a simple (in concept) core polarization model largely developed by Drachman (1993). An examination of the eigenvalues for Rydberg states reveals two significant features. First, with increasing L, the first several figures are accounted for by the screened hydrogenic energy

$$E_{\rm SH}=-\frac{Z^2}{2}-\frac{(Z-1)^2}{2n^2} \tag{12}$$

corresponding to the energy of the inner $1s$ electron with the full nuclear charge Z, and the outer nl electron with the screened nuclear charge $Z-1$. Second, the singlet-triplet splitting goes rapidly to zero with increasing L. This suggests that for sufficiently high L, one can

[4]See the *Atomic, Molecular, and Optical Physics Handbook* (Drake, 1996), which includes a number of articles discussing computational techniques for the few- and many-body problems in detail, and which includes many important earlier references.

TABLE II. Asymptotic expansion for the energy of the $1s10k$ state of helium.

Quantity	Value
$-Z^2/2$	−2.000 000 000 000 000 00
$-1/(2n^2)$	−0.005 000 000 000 000 00
$c_4\langle r^{-4}\rangle$	−0.000 000 007 393 341 95
$c_6\langle r^{-6}\rangle$	0.000 000 000 004 980 47
$c_7\langle r^{-7}\rangle$	0.000 000 000 000 278 95
$c_8\langle r^{-8}\rangle$	−0.000 000 000 000 224 33
$c_9\langle r^{-9}\rangle$	−0.000 000 000 000 002 25
$c_{10}\langle r^{-10}\rangle$	0.000 000 000 000 003 73
Second order	−0.000 000 000 000 070 91
Total	−2.005 000 007 388 376 30(74)
Variational	−2.005 000 007 388 375 8769(0)
Difference	−0.000 000 000 000 000 42(74)

treat the Rydberg electron as a distinguishable particle moving in the field of the polarizable core consisting of the nucleus and the tightly bound $1s$ electron. The various multipole moments of the core then give rise to an asymptotic potential of the form

$$\Delta V(r)=\frac{c_4}{r^4}+\frac{c_6}{r^6}+\frac{c_7}{r^7}+\cdots, \tag{13}$$

where r is the coordinate of the Rydberg electron. In first order, the correction to the energy is then $\langle\Delta V(r)\rangle$, where the expectation value is with respect to the Rydberg electron. Since the core is a hydrogenic system, all the c_i coefficients and expectation values can be calculated analytically. For example, c_4 is related to the core polarizability $\alpha_1=(9/32)a_0^3$ by $c_4=-\alpha_1/2$ (a_0 is the Bohr radius), and c_6 is related to the quadrupole polarizability $\alpha_2=(15/64)a_0^5$ and a nonadiabatic correction to the dipole polarizability $\beta_1=(43/512)a_0^5$ by $c_6=-\alpha_2/2+3\beta_1$. Detailed expressions for the higher-order terms up to c_{10} have been derived [see Drachman (1993) for further discussion]. Each term can be calculated analytically by repeated use of the perturbation methods of Dalgarno and Lewis (1956). However, the expansion must be terminated at $i=(L+1)$ because the expectation values $\langle r^{-i}\rangle$ diverge beyond this point. In this sense, the series must be regarded as an asymptotic expansion.

As an example, Table II shows that the terms up to c_{10}, together with a second-order perturbation correction, account for the variationally calculated energy of the $1s10k$ state to within an accuracy of only a few Hz. All the entries can be expressed analytically as rational fractions. For example, the $c_4\langle r^{-4}\rangle$ contribution is exactly (in atomic units)

$$c_4\langle r^{-4}\rangle=-\frac{3\times 61}{2^{10}\times 5^6\times 7\times 13\times 17}$$
$$=-7.39334195\cdots\times 10^{-9}. \tag{14}$$

Since the accuracy of the symptotic expansion rapidly gets even better with increasing L, there is clearly no need to perform numerical solutions to the Schrödinger equation for $L>7$. The entire singly excited spectrum of helium is covered by a combination of high-precision variational solutions for small n and L, quantum defect extrapolations for high n, and asymptotic expansions based on the core polarization model for high L.

Asymptotic expansion methods have similarly been applied to the Rydberg states of lithium and compared with high-precision measurements (Bhatia and Drachman, 1997). This case is more difficult because the Li^+ core is a nonhydrogenic two-electron ion for which the multipole moments cannot be calculated analytically, and variational basis-set methods must be used instead. However, the method is in principle capable of the same high accuracy as for helium.

3. Relativistic and QED effects

The accuracy of the foregoing results for helium exceeds that of the best measurements by a wide margin. However, numerous small corrections must be added before a meaningful comparison with experiment can be made. Many of these can also be calculated to high precision, leaving a finite residual piece due to higher-order relativistic and quantum-electrodynamic effects which lie at the frontier of current theory.

The two relevant parameters in calculating corrections to the nonrelativistic energy for infinite nuclear mass are μ/M and α, where $\mu=m_eM/(m_e+M)$ is the reduced electron mass and α is the fine-structure constant. Since $\mu/M\approx 1.3707\times 10^{-4}$ for helium, and $\alpha^2\approx 0.5328\times 10^{-4}$, these terms are the same order of magnitude. The expansion then has the form (in units of e^2/a_μ)

$$E=E_0^0+E_0^1(\mu/M)+E_0^2(\mu/M)^2+E_2^0\alpha^2$$
$$+E_2^1\alpha^2(\mu/M)+E_3^0\alpha^3+\cdots. \tag{15}$$

The leading terms can be expressed as expectation values and accurately calculated. For example, $E_0^1=-\langle\Delta_1\cdot\Delta_2\rangle$ is the specific mass shift due to the mass polarization operator, and E_0^2 is the second-order perturbation correction. The leading relativistic term E_2^0 is the expectation value of the well-known Breit operator (Bethe and Salpeter, 1957) for infinite nuclear mass, but the finite-mass correction E_2^1 contains new operators coming from a systematic reduction of the pairwise Breit interactions in the full three-body problem to center-of-mass plus relative coordinates along with mass scaling and mass polarization contributions. Although these terms become increasingly complicated, they can still be accurately calculated and subtracted from measured transition frequencies.

The leading QED term E_3^0 is the first term to present new computational challenges. It contains contributions coming from both the electron-nucleus interactions of leading order α^3Z^4 and the electron-electron interaction of leading order α^3Z^3. The general form of the electron-nucleus part $E_{3,Z}^0$ for helium is simply obtained from the corresponding hydrogenic case by inserting the correct

electron density at the nucleus in place of the hydrogenic quantity $\langle\delta(\mathbf{r})\rangle = Z^3/(\pi n^3)$. This part is easily done, but the Bethe logarithm $\beta(nLS)$, representing the emission and absorption of virtual photons, is much more difficult to calculate. It is defined in terms of a sum over virtual two-electron intermediate states,

$$\beta(nLS) = \frac{\Sigma_m |\langle 0|\mathbf{p}_1+\mathbf{p}_2|m\rangle|^2 (E_m - E_0)\ln[2Z^{-2}(E_m - E_0)]}{\Sigma_m |\langle 0|\mathbf{p}_1+\mathbf{p}_2|m\rangle|^2 (E_m - E_0)}. \tag{16}$$

The accurate calculation of $\beta(nLS)$ is one of the most challenging problems in atomic structure theory. The problem is that the sum in the numerator is very nearly divergent, and so the dominant contribution comes from states lying high in the scattering continuum (both one- and two-electron). In a monumental calculation based on earlier work by Schwartz (1961), Baker *et al.* (1993) have obtained accurate values of $\beta(nLS)$ for the low-lying S states of helium (1^1S, 2^1S, and 2^3S). These results have an important impact on bringing theory and experiment into agreement.

Although no other direct calculations of similar accuracy are available for other states, for sufficiently high L one can use instead the core polarization model. This picture shows that the dominant contribution to the change in $\beta(nLS)$ from the hydrogenic $\beta(1s)$ comes from the perturbing effect of the Rydberg electron on the $1s$ electron, rather than from the Rydberg electron itself. The dipole polarization result allows $\beta(nLS)$ to be expressed in terms of the known hydrogenic Bethe logarithms, plus a correction term proportional to $\langle r^{-4}\rangle_{nl}$ calculated with respect to the screened hydrogenic wave function of the Rydberg electron. This result is of pivotal importance because it allows the QED part of the D-state energies to be calculated to sufficient accuracy that these states can be taken as absolute points of reference in the interpretation of measured transition frequencies. In particular, the much larger S-state QED shift can then be extracted from measured nS-$n'D$ transition frequencies by subtraction of the other known terms.

Relativistic and QED terms of order α^4 a.u. and α^5 a.u. are also important in the comparison with experiment. The theory of these terms is incomplete. A complete treatment requires a systematic reduction of the Bethe-Salpeter equation in order to find equivalent nonrelativistic operators whose expectation values in terms of Schrödinger wave functions yield the correct coefficients for a given order of α. The result then represents an extension of the Breit interaction to higher order. To date, this ambitious program has been carried to completion only for the spin-dependent parts (see Sec. V.B.4). However, a comparison with experiment indicates that for S states, these higher-order terms are dominated by large QED contributions analogous to the corresponding terms in the one-electron Lamb shift. For example, the term $E^0_{4,Z}$ or order α^4 contributes to -771.1 MHz, -51.995 MHz, and -67.634 MHz, respectively, to the (positive) ionization energies of the helium $1s^2\,{}^1S$, $1s2s\,{}^1S$, and $1s2s\,{}^3S$ states, while the experimental uncertainties are more than an order of magnitude smaller. There would be large discrepancies between theory and experiment without this QED term. The comparison between theory and experiment [see Drake and Martin (1998)] shows that, for the ionization energy of the $1s^2\,{}^1S$ ground state of helium, the two agree at the ± 100 MHz level (1.7 parts in 10^8) out of a total ionization energy of 5 945 204 226(100) MHz. The total QED contribution is $-41\,233(100)$ MHz. For the $1s2s\,{}^1S$ state, the agreement is spectacularly good. The difference between theory and experiment is only 1.1 MHz (1.2 parts in 10^9) out of a total ionization energy of 960 332 040 MHz. Both of these results rely on the calculated ionization energies of the higher-lying P- and D-state energies as absolute points of reference.

4. Fine-structure splittings and the fine-structure constant

The helium $1s2p\,{}^3P$ manifold of states has three fine-structure levels labeled by the total angular momentum $J=0$, -1, and 2. If the largest $J=0\rightarrow 1$ interval of about 29 617 MHz could be measured to an accuracy of ± 1 kHz, this would determine the fine-structure constant α to an accuracy of ± 1.7 parts in 10^8, provided that the interval could be calculated to a similar degree of accuracy. This degree of accuracy would provide a significant test of other methods of measuring α, such as the ac Josephson effect and the quantum Hall effect, where the resulting values of α differ by 15 parts in 10^8 (Kinoshita and Yennie, 1990). Groups are now working toward the achievement of a ± 1 kHz measurement of the fine-structure interval.

Theory is also close to achieving the necessary accuracy. In lowest order, the dominant contribution of order α^2 a.u. comes from the spin-dependent part of the Breit interaction. This part is known to an accuracy of better than 1 part in 10^9, and corrections of order α^3 a.u. and α^4 a.u. have similarly been calculated to the necessary accuracy. At each stage, the principal challenge is to find the equivalent nonrelativistic operators whose expectation value in terms of Schrödinger wave functions gives the correct coefficient of the corresponding power of α. This analysis has been completed for the next higher-order $\alpha^5 \ln\alpha$ and α^5 terms, and numerical results obtained for the former. A full evaluation of the remaining α^5 terms should be sufficient to reduce the theoretical uncertainty from the present ± 20 kHz to less than 1 kHz. Once both theory and experiment are in place to

the necessary accuracy, a new value of α can be derived. At present, theory and experiment agree at the ± 20-kHz level (Storry and Hessels, 1998). This already represents a substantial advance in the accuracy that can be achieved for spin-dependent effects on helium.

C. Theory of few-electron ions

In the foregoing discussion of helium, the starting point was the nonrelativistic Schrödinger equation with relativistic and QED effects treated by successive orders of perturbation theory. However, measurements of transition frequencies are available for many He-like ions all the way up to two-electron uranium (U^{90+}). For such high-Z systems, relativistic effects predominate and a perturbation expansion in powers of αZ is no longer appropriate. On the other hand, electron correlation effects decrease in proportion to $1/Z$ relative to the one-electron energies due to the dominant Coulomb field of the nucleus. This suggests that one should start instead from the one-electron Coulomb-Dirac equation so that relativistic effects are included to all orders from the beginning, and treat electron correlation effects by perturbation theory. As a rough rule of thumb, the high-Z region begins when relativistic effects become larger than electron correlation effects, i.e., when $(\alpha Z)^2 > 1/Z$, or $Z > 26$.

The so-called Unified Method (Drake, 1988) provides a quick and simple way to merge $1/Z$ expansions for the nonrelativistic part of the energy with exact Dirac energies [i.e., $(\alpha Z)^2$ expansions summed to infinity] for the relativistic part. With allowance for QED corrections, the resulting energies are remarkably accurate over the entire range of nuclear charge. However, the accuracy of recent measurements for high-Z ions has now reached the point that higher-order contributions arising from the combined effects of relativity and electron correlation become important. The leading such term not included by the Unified Method is of order $(\alpha Z)^4$ a.u. and $\alpha^4 Z^2$ relative to the nonrelativistic energy. Terms of this order are automatically included in much more elaborate calculations based on the techniques of relativistic many-body perturbation theory and relativistic configuration interaction [see Sapirstein (1998) for a review]. Especially important are methods for evaluating all orders of perturbation theory at once. Although these methods are less accurate than the nonrelativistic Hylleraas-type calculations for the neutral helium and lithium atoms and their isoelectronic low-Z ions, they yield good agreement with experiment for intermediate- and high-Z ions. There is a broad range of Z between about 6 and 40 where both approaches yield results of useful accuracy and allow interesting comparisons between them.

D. Future prospects

The results described here indicate the high degree of understanding that has been achieved for few-electron systems over the entire range of nuclear charge from neutral atoms to highly ionized uranium. For the heliumlike systems, the Schrödinger equation has been solved and lowest-order relativistic corrections calculated to much better than spectroscopic accuracy. To a somewhat lesser extent, accurate solutions also exist for lithiumlike systems.

For highly ionized systems, many-body perturbation theory and relativistic CI provide powerful computational techniques. The residual discrepancies between theory and experiment determine the higher-order relativistic and QED (Lamb shift) contributions to nearly the same accuracy as in the corresponding hydrogenic systems. Interest therefore shifts to the calculation of these contributions, for which theory is far from complete for atoms more complicated than hydrogen. New theoretical formulations are needed, such as the simplifications recently discussed by Pachucki (1998). Each theoretical advance provides a motivation for parallel advances in the state of the art for high-precision measurement. The results obtained to date provide unique tests of both theory and experiment at the highest attainable levels of accuracy, and they point the way to applications to more complex atoms and molecules.

VI. EXOTIC ATOMS

G. zu Putlitz

"Exotic atoms" such as positronium and muonium are pure leptonic hydrogenlike systems perfectly suited for testing the electromagnetic interaction and possible tiny admixtures of other interactions like the weak and strong force or possible unknown forces beyond the standard model. The progress made in this field up to now has produced experimental values of such precision that the results and their interpretations compete with the experiments of elementary particle physics carried out at the highest energies available so far.

Of major importance are atoms with negatively charged particles in the atomic shell, particularly those with a negative muon.

The production of exotic atoms relies on the production of exotic particles with suitable intensity, phase space, and energy to be captured by a normal atom. For muonic atoms with a negative muon, formation initially involved a proton beam with energies of 0.5 to 2.0 GeV striking a target to produce negative pions. The π^- decay with a lifetime of $\tau_\pi = 2.6 \times 10^{-8}$ sec through the reaction $\pi^- \rightarrow \mu^- + \overline{\nu}_\mu$. The negative muons are subsequently decelerated by propagation through matter until they reach energies at which they are captured in states with rather high principal and orbital angular momentum quantum numbers. In the beginning of the capture process the energy is mostly released by Auger ionization of outer-shell electrons. Later on the muons reach lower states by emission of electromagnetic radiation with discrete energies. This part of the spectrum is particularly important not only for the investigation of the

atomic potential but also for a measurement of the mass of the muon. In lower orbits the negative muons interact directly with the nucleus and annihilate through the weak interaction.

The electromagnetic spectrum emitted from a muon captured in an atom results in the emission of γ radiation where the energy levels E_n are

$$E_n = -\frac{\mu_{\text{red}} c^2}{2}\left(\frac{Z\alpha}{n}\right)^2. \tag{17}$$

The corresponding Bohr radius is

$$\tau_n = \frac{\hbar^2}{\mu_{\text{red}} e^2}\frac{n^2}{Z}, \tag{18}$$

where n is a principal quantum number of the state, μ_{red} is the reduced mass of the negative particle X in the shell Z = nuclear charge number, and $\alpha = (e^2/\hbar c)$ = fine-structure constant $\approx \frac{1}{137}$. For a medium-mass nucleus the energy for the muonic Lyman-α line (10.2 eV for the electron in hydrogen) is in the MeV range. The corresponding orbit of the muon is located well inside the electronic shells for lower principal quantum numbers. The measured energy in this case is smaller than the point-charge value estimated above because of the different potential the μ^- experiences close to the nuclear surface. The Bohr radius and the nuclear radii become comparable.

Muonic x rays were first measured by Fitch and Rainwater in 1953. Over the decades the precision in muonic atom spectroscopy (as well as that for pionic, kaonic, and other spectra) has increased greatly due to increased beam intensities, the availability of solid-state detectors, and the construction of special crystal-diffraction spectrometers. Extensive data have been obtained on the energies of muonic spectra, which have led to the measurement of nuclear radii, of isotope and isotone displacements of muonic lines, and the change of the charge distribution of isomeric nuclei.

For larger nuclear charges, radiative corrections and corrections for effects of nuclear polarization are significant. Nevertheless, the spectra of pionic, kaonic, and hadronic atoms have played a very important role in the study of systematic trends of the charge and mass distribution in nuclei as well as nuclear deformations over large sequences of isotopes.

From the measurement of several transitions in a particular muonic atom at least two parameters of the charge distribution can be determined, the mean charge radius C and the skin thickness of the charge distribution t. In addition the width of the energy levels measured through the linewidth of the γ transition can be used to measure the rate of absorption processes of the exotic particles in the nucleus. For muonic hydrogen in the $1S$ state this rate is rather small compared to the natural decay rate of the muon of $R \approx (1/\tau_\mu) \approx 5\times 10^5$ s^{-1} but has been measured rather precisely to be $R_c \approx 500$ s^{-1}. For lower nuclear charge numbers the capture probability for the muon by the nucleus increases with Z^4. For this reason even at relatively low Z capture processes dominate the linewidth of lower muonic transitions.

Muonic helium is an exotic atom with special features. It is produced by a capture reaction in which both of the electrons are emitted by the Auger effect. The remaining $(He^{++}\mu^-)^+$ ion has a hydrogenlike spectrum and can capture an electron in the same way as does a proton. Its term energies have been recorded through soft γ-ray spectroscopy (in which the energy of the Lyman-α line = 8.2 keV) and its fine structure was investigated in a laser experiment. A decade later neutral $(He^{++}\mu^- e^-)^0$ atoms were produced and the hyperfine structure was measured with high precision (Hughes, 1990). This atomic system is very peculiar because it constitutes a hydrogen atom within a hydrogen atom. Table III lists the negative exotic particles that are suitable for the production of exotic atoms. Tauonic atoms have not been observed so far because the lifetime of the τ lepton of 10^{-13} s is very short, and the probability of annihilation by nuclear absorption is very large.

Antiprotonic atoms are also formed by the capture of antiprotons into states with large quantum numbers. The spectra recorded for antiprotonic hydrogen, He, and other light atoms correspond, for large quantum numbers, to the theoretical predictions based on electromagnetic forces. However, for smaller quantum numbers the strong interaction starts to dominate and a strongly bound system, protonium $\bar{p}p$, is formed which annihilates very rapidly via the strong interaction into hadrons.

The study of antiprotonic atoms was stimulated by the discovery that some of the highly excited states in antiprotonic neutral helium $^4He^+\bar{p}^- e^-$ have a rather long lifetime (Yamazaki, 1992). This fact was utilized to investigate via laser spectroscopy transitions between states of quantum numbers around $n = 35$ and the highest possible orbital angular momentum quantum numbers.

The investigation of neutral antimatter with high precision has been a target of scientific investigation for many decades, promoted by the synthesis of antideuterons some 30 years ago. With our present knowledge the strong electromagnetic and weak forces have to be considered as equal for matter and antimatter, but the question of the gravitational equality of matter and antimatter remains unsettled. For this reason, and also to achieve a more sensitive test of CPT invariance, the production of neutral antihydrogen ($\bar{H} = \bar{p}e^+$) is being actively pursued following three different pathways. These are (1) the storage of antiprotons and positrons in the same trap volume and obtaining $\bar{H}$ by three-body collisions; (2) laser-induced recombination of parallel $\bar{p}$ and e^+ beams of the same velocity from continuum states[5]; and (3) production of $\bar{p}$ and e^+ in the same phase space

[5]See also the discussion of electron-ion recombination in Sec. III.C.

TABLE III. Properties of nonstable leptons, mesons, hadrons and antiprotons (all with $Z=-1$).

Particle	Mass m [MeV]	Mean lifetime $\tau[s]$	Bohr energy [KeV] $E_B=E_0\frac{m}{m_e}z^2$	Bohr radius $a_B=\frac{m_e}{m}\frac{a_0}{Z}$ [fm]
μ^-	106	2.2×10^{-6}	$2.8\times Z^2$	$255/Z$
τ^-	1784	2.9×10^{-13}	$47.5\times Z^2$	$15/Z$
π^-	140	2.6×10^{-8}	$3.7\times Z^2$	$193/Z$
K^-	494	1.2×10^{-8}	$13.1\times Z^2$	$55/Z$
Σ^-	1197	1.5×10^{-10}	$31.8\times Z^2$	$23/Z$
Ξ^-	1321	1.6×10^{-10}	$35.2\times Z^2$	$21/Z$
Ω^-	1673	0.8×10^{-10}	$44.5\times Z^2$	$16/Z$
$\bar{p}$	938	∞	$25.0\times Z^2$	$29/Z$

with simultaneous binding of oppositely charged particles. The latter method was successful in detecting antihydrogen at high energy. However, it is not well suited for precision measurements on antihydrogen. The forthcoming experiments with $\bar{H}$ in traps may clarify this interesting basic question about gravitation.

Positronium and muonium are prominent examples of the wealth of information which can be obtained from these exotic atoms. Positronium was discovered by M. Deutsch and collaborators (1951) and has been investigated with ever increasing precision with respect to its term energies and decay constants in the different angular momentum coupling states. Positronium is formed if positrons from a source (e.g., ^{22}Na, ^{64}Cu) are stopped in a gas or in a fine dispersed powder. Positron-electron capture results in two states, 1^1S_0 (parapositronium) and 1^3S_1 (orthopositronium). The decay of positronium is governed by C parity conservation, which requires that parapositronium decay collinearly into γ quanta with the energy of the rest mass of the electron $E_\gamma=511\,\mathrm{KeV}$ and the lifetime $\tau(^1S_0)=1.25\times10^{-10}$ s. The $^3S_1$ state (orthopositronium) decays predominantly via 3γ quanta and has a lifetime of $\tau(^3S_1)=1.4\times10^{-7}$ s. The difference in decay modes and lifetimes makes possible high-precision spectroscopic measurements of the energy difference between $^1S_0$ and $^3S_1$. After the fast decay of the $^1S_0$ state formed initially, radio-frequency transitions into this state from the $^3S_1$ increase the number of two-quantum decays and thus provide a signal. Positronium is an ideal system in which to study quantum electrodynamics and radiative corrections. The splitting ΔE of the ground state can be written in lowest order as

$$\Delta E(1^3S_1-1^1S_0)=\left(\frac{4}{6}+\frac{3}{6}\right)\alpha^2R_\infty, \tag{19}$$

where R_∞ is the Rydberg constant.

The latest values for splitting are $\Delta E(1^3S_1-1^1S_0)_{\mathrm{theor}}=2.03380\times10^{11}\,\mathrm{Hz}$ and $\Delta E(1^3S_1-1^1S_0)_{\mathrm{exp}}=2.03398(11)\times10^{11}\,\mathrm{Hz}$, are in satisfactory agreement. The annihilation rates are a further test of the electromagnetic interaction. The corresponding results for the lifetime of the $^1S_0$ state are in adequate agreement, $\tau_{\mathrm{theor}}=0.79854(36)\times10^{10}\ \mathrm{s}^{-1}$ and $\tau_{\mathrm{exp}}=0.799(11)\times10^{10}\ \mathrm{s}^{-1}$. However for the 1^3S_1 state, the results $\tau^{-1}_{\mathrm{exp}}=0.7262(15)\times10^7\ \mathrm{s}^{-1}$ and $\tau_{\mathrm{theor}}=0.72119(39)\times10^7\ \mathrm{s}^{-1}$ disagree substantially (Mills and Chu, 1990).

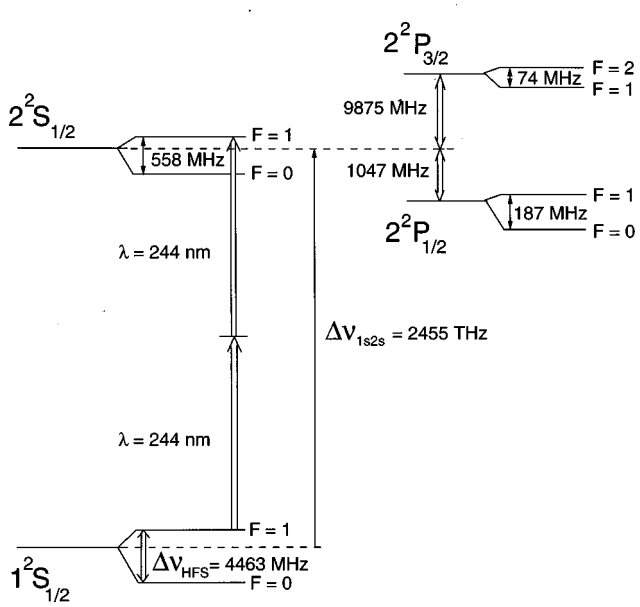

FIG. 6. Level scheme of muonium for the two first main quantum numbers $n=1$ and $n=2$. Double arrows indicate those transitions which have been measured experimentally so far.

Like positronium, muonium is also a pure leptonic atom dominated by the electromagnetic interaction between the particles. Since pair annihilation cannot take place between two unequal leptons, muonium (μ^+e^-) is much more longer lived than positronium. Its lifetime is determined by the lifetime of the positive muon $\tau(\mu^+)=2.19703(4)\times10^{-6}$ s. This rather long lifetime makes muonium very suitable for high-precision experiments. The spectrum of muonium in its ground and first excited states (Fig. 6) shows which measurements are possible and desirable. The hyperfine-structure splitting of the ground state can be written in lowest order as

$$\Delta\nu_{hfs}=\left(\frac{16}{3}\alpha^2cR_\infty\frac{\mu_\mu}{\mu_0}\right)\left(1+\frac{m_e}{m_\mu}\right)^3. \tag{20}$$

Measurements in zero, weak, and strong magnetic fields can be utilized to extract the magnetic moment of the muon and the fine-structure constant.

Muonium was discovered by Hughes and collaborators (Hughes *et al.*, 1960) when positive muons were stopped in highly purified argon gas. Muons are produced by the decay of pions in a two-body decay via the weak interaction. Consequently they exhibit spin polarization with respect to their momentum. Since the capture process of the electron does not destroy this polarization, muonium is polarized. The subsequent weak decay into positrons and neutrinos shows a $(\mathbf{1}+\cos\theta)$-positron distribution with respect to the muon spin direction, which can be used to detect the μ^+ polarization at the time of the decay. Consequently spin depolarizing radio-frequency transitions can be detected

through the change in the e^+ decay angular distribution (Hughes and zu Putlitz, 1990). After some 35 years of research the value of the hyperfine splitting in muonium $\Delta\nu_{hfssls}(\mathrm{M})$ has been improved from 4461.3 (2.2) MHz to 4463.302764 (54) MHz.

The mass of the muon can be determined from a measurement of the energy difference between the $1S$ and $2S$ levels. The method of collinear two-photon laser spectroscopy between the $1^2S_{1/2}-2^2S_{1/2}$ states at $\lambda = 244\,\mathrm{nm}$ and the subsequent ionization by a third quantum of the same light field resulted in a best value for the splitting $\Delta\nu(1^2S_{1/2}-2^2S_{1/2}) = 2\,455\,529\,002\,(33)\,(46)$ MHz. It should be mentioned also that muonium has been used to measure the Lamb shift in the $n=1$ and $n=2$ states and the fine-structure splitting $2^2P_{1/2}-2^2P_{3/2}$.

The formation and synthesis of the pionium atom II $=(\pi^+e^-)$ have been observed. The pion has no spin and pionium no hyperfine structure, but the $n=1-n=2$ transition is attractive for an investigation of the pion form factor. An experiment to observe this transition can possibly be made in the future if larger intensities of such particles are available. Obviously high intensities of exotic particles open the way also to artificial bound systems containing two unstable particles like $\mu^+\mu^-$, $\pi^+\pi^-$, $K^+\pi^-$, and K^+K^-, as well as many other combinations. The $\pi^+\mu^-$ atom has been detected from the decay $K_L^0\rightarrow\pi\mu\nu$ where π and μ were emitted with the same velocity and in a small solid angle (Coombes *et al.*, 1973). Another five orders of magnitude in the flux of muons possibly available in a muon collider would result in unprecedented possibilities with low-energy high-intensity muon beams.

Exotic atoms have contributed to our understanding of exotic particles and their binding in an atom, as well as to our knowledge of the structure and deformation of atomic nuclei. Simple pure leptonic and hydrogenlike exotic atoms have provided some of the most precise tests of quantum electrodynamics in bound systems. In simple systems of bound elementary particles, fundamental symmetries in physics have been tested. Exotic atom spectroscopy will continue in the future to be a highly exciting field of research.

ACKNOWLEDGMENTS

V. W. Hughes contributed significantly to the preparation of this article. Research support of G.W.F.D. by the Natural Sciences and Engineering Research Council of Canada is gratefully acknowledged.

REFERENCES

Accad, Y., C. L. Pekeris, and B. Schiff, 1971, Phys. Rev. A **4**, 516, and earlier references therein.

Alguard, M. J., V. W. Hughes, M. S. Lubell, and P. F. Weinwright, 1977, Phys. Rev. Lett. **39**, 334.

Amaldi, U., R. Egidi, R. Marconero, and G. Pizzela, 1969, Rev. Sci. Instrum. **40**, 1001.

Andersen, N., I. V. Hertel, and H. Kleinpoppen, 1984, J. Phys. B **24**, L901.

Andersen, N., J. W. Gallagher, and I. V. Hertel, 1988, Phys. Rep. **165**, 1.

Andersen, N., J. T. Broad, E. E. B. Campbell, J. W. Gallagher, and I. V. Hertel, 1997, Phys. Rep. **278**, 107.

Atomic Physics 16: Proceedings of the 16th International Conference on Atomic Physics (ICAP), 1997 (University of Windsor, Windsor, Ontario, Canada).

Aumayr, F., and H. Winter, 1998, Eds., *Photonic, Electronic and Atomic Collisions: Invited Papers of the 20th International Conference*, Vienna, 1997 (World Scientific, Singapore).

Awe, B., F. Kemper, F. Rosicky, and R. Feder, 1983, J. Phys. B **16**, 603.

Baker, J. D., R. C. Forrey, J. D. Morgan, R. N. Hill, M. Jeziorska, and J. Schertzer, 1993, Bull. Am. Phys. Soc. **38**, 1127.

Baker, J. D., D. E. Freund, R. N. Hill, and J. D. Morgan III, 1990, Phys. Rev. A **41**, 1247.

Bederson, B., 1969, Comments At. Mol. Phys. **1**, 41 and 65.

Bederson, B., 1970, Comments At. Mol. Phys. **2**, 160.

Bederson, B., and W. L. Fite, 1968, Eds., *Atomic and Electron Physics: Atomic Interactions*, Methods of Experimental Physics No. 7 (Academic, New York).

Berger, O., and J. Kessler, 1986, J. Phys. B **19**, 3539.

Bethe, H. A., and E. E. Salpeter, 1957, *Quantum Mechanics of One- and Two-Electron Atoms* (Springer-Verlag, New York).

Bhatia, A. K., and R. J. Drachman, 1997, Phys. Rev. A **55**, 1842.

Blum, K., 1996, *Density Matrix Theory and Applications*, second edition (Plenum, New York/London).

Born, M., and E. Wolf, 1970, *Principles of Optics* (Pergamon, Oxford).

Bransden, B. H., 1983, *Atomic Collision Theory* (Benjamin/Cummings, Reading, MA).

Bürgers, A., D. Wintgen, and J.-M. Rost, 1995, J. Phys. B **28**, 3163.

Burke, P. G., 1965, Adv. Phys. **14**, 521.

Burke, P. G., and C. J. Joachain, 1995, *The Theory of Electron-Atom Collisions* (Plenum, New York/London).

Burke, P. G., and H. M. Schey, 1962, Phys. Rev. **126**, 147.

Condon, E. U., and G. H. Shortley, 1935, *The Theory of Atomic Spectra* (Cambridge University, Cambridge, England).

Coombes, R., *et al.*, 1973, Phys. Rev. Lett. **37**, 249.

Dalgarno, A., and J. T. Lewis, 1956, Proc. R. Soc. London, Ser. A **233**, 70.

Dalgarno, A., and A. L. Stewart, 1956, Proc. R. Soc. London, Ser. A **238**, 269.

Datz, S., and P. F. Dittner, 1988, Z. Phys. D **10**, 187.

Deutsch, M., 1951, Phys. Rev. **82**, 455.

Drachman, R. J., 1993, in *Long-Range Casimir Forces: Theory and Recent Experiments on Atomic Systems*, edited by F. S. Levin and David Micha (Plenum, New York), p. 219, and earlier references therein.

Drake, G. W. F., 1988, Can. J. Phys. **66**, 586.

Drake, G. W. F., 1993a, Adv. At., Mol., Opt. Phys. **31**, 1; 1994, *ibid.* **32**, 93.

Drake, G. W. F., 1993b, in *Long-Range Casimir Forces: Theory and Recent Experiments on Atomic Systems*, edited by F. S. Levin and D. A. Micha (Plenum, New York), p. 107.

Drake, G. W. F., 1996, Ed., *Atomic, Molecular, and Optical Physics Handbook* (AIP, New York).

Drake, G. W. F., 1998, in *Encyclopedia of Applied Physics*, edited by George L. Trigg (Wiley-VCH, Weinheim/New York), Vol. 23, p. 121.
Drake, G. W. F., and W. C. Martin, 1998, Can. J. Phys. **76**, 597.
Duké, L. J., J. B. A. Mitchell, J. W. McConkey, and C. E. Brion, 1996, Eds., *19th International Conference on the Physics of Electronic and Atomic Collisions*, Whistler, B.C., Canada, 1995, AIP Conf. Proc. No. 360 (AIP, New York).
Ehrhardt, H., M. Schulz, T. Tekaat, and K. Willmann, 1969, Phys. Rev. Lett. **22**, 89.
Eminyan, M., K. B. MacAdam, J. Slevin, and H. Kleinpoppen, 1973, Phys. Rev. Lett. **31**, 576.
Eminyan, M., K. B. MacAdam, J. Slevin, and H. Kleinpoppen, 1974, J. Phys. **12**, 1519.
Fano, U., 1957, Rev. Mod. Phys. **29**, 74.
Fano, U., 1973, Rev. Mod. Phys. **45**, 553.
Fano, U., and J. Macek, 1973, Rev. Mod. Phys. **45**, 553.
Farago, P., 1974, J. Phys. B **7**, L28.
Farago, P., 1976, *Electron and Photon Interactions with Atoms* (Plenum, New York/London), p. 235.
Fitch, V. L., and J. Rainwater, 1953, Phys. Rev. **92**, 789.
Fite, W. L., and R. T. Brackmann, 1958, Phys. Rev. **112**, 1151.
Fock, V., 1930, Z. Phys. **61**, 126.
Gallager, A., 1996, in *Atomic, Molecular, and Optical Physics Handbook*, edited by G. W. F. Drake (AIP, New York).
Goldman, S. P., 1998, Phys. Rev. A **57**, R677.
Haberland, R., L. Fritsche, and J. Noffke, 1986, Phys. Rev. A **33**, 2305.
Hafner, H., H. Kleinpoppen, and H. Krüger, 1965, Phys. Lett. **18**, 270.
Hanne, G. F., 1996a, Can. J. Phys. **74**, 811.
Hanne, G. F., 1996b, in *Selected Topics on Electron Physics*, edited by D. M. Campbell and H. Kleinpoppen (Plenum, New York/London), p. 57.
Hartree, D. R., 1928, Proc. Cambridge Philos. Soc. **24**, 89, 111.
Heinzen, D. J., 1996, in *Atomic Physics 14*, Proceedings of the 14th International Conference on Atomic Physics, 1995, edited by S. J. Smith, D. J. Wineland, and C. E. Wieman, AIP Conf. Proc. No. 323 (AIP, New York).
Heinzmann, U., and N. A. Cherepkov, 1996, in *VUV and Soft X-ray Photoionization*, edited by U. Becker and D. A. Shirley (Plenum, New York).
Hertel, I. V., and H. Stoll, 1974, J. Phys. B **7**, 570.
Hils, D., and H. Kleinpoppen, 1978, J. Phys. B **11**, L283.
Hils, D., V. McCusker, H. Kleinpoppen, and S. J. Smith, 1972, Phys. Rev. Lett. **29**, 398.
Hippler, R., H. Madeheim, W. Harbich, H. Kleinpoppen, and H. O. Lutz, 1988, Phys. Rev. A **38**, 1662.
Hughes, V. W., and G. zu Putlitz, 1990, in *Quantum Electrodynamics*, edited by T. Kinoshita (World Scientific, Singapore), p. 822.
Hughes, V. W., *et al.* 1960, Phys. Rev. Lett. **5**, 63.
Hylleraas, E. A., 1963, Rev. Mod. Phys. **35**, 421.
Jetzke, S., J. Zaremba, and F. H. M. Faisal, 1989, Z. Phys. D **11**, 63.
Joachain, C. J., 1983, in *Quantum Collision Theory* (North-Holland, Amsterdam).
Kinoshita, T., and D. R. Yennie, 1990, in *Quantum Electrodynamics*, edited by T. Kinoshita (World Scientific, Singapore), p. 1.
Klar, H., and H. Kleinpoppen, 1982, J. Phys. B **15**, 933.
Klar, H., A. C. Roy, P. Schlemmer, K. Jung, and H. Ehrhardt, 1987, J. Phys. B **20**, 821.
Kleinpoppen, H., and V. Raible, 1965, Phys. Lett. **18**, 24.
Krause, H. F., and S. Datz, 1996, in *Advances in Atomic, Molecular, and Optical Physics*, edited by B. Bederson and H. Walther (Academic, New York), Vol. 26, p. 139.
Larsson, M., 1995, Rep. Prog. Phys. **58**, 1267.
Macek, J., and D. H. Jaecks, 1971, Phys. Rev. A **4**, 1288.
Madden, R. P., and K. Codling, 1963, Phys. Rev. Lett. **10**, 516.
Marton, L. L., and Patrick Richard, 1980, Eds., *Atomic Physics; Accelerators*, Methods of Experimental Physics No. 17 (Academic, New York).
Massey, H. S. W., 1942, Proc. R. Soc. London, Ser. A **181**, 14.
Massey, H. S. W., 1979, *Atomic and Molecular Collisions* (Taylor and Francis, London).
McCarthy, I. E., and E. Weigold, 1991, Rep. Prog. Phys. **54**, 789.
McDaniel, E. W., 1989, *Atomic Collisions* (Wiley, New York).
McEachran, R. P., and A. D. Stauffer, 1986, J. Phys. B **19**, 3523.
Merzbacher, E., 1998, *Quantum Mechanics*, 3rd edition (Wiley, New York), Chap. 13.
Miller, J. D., R. A. Cline, and D. J. Henzen, 1993, Phys. Rev. Lett. **71**, 2204.
Mills, A. P., Jr., and S. Chu, 1990, in *Quantum Electrodynamics*, edited by T. Kinoshita (World Scientific, Singapore), p. 774.
Mott, N. F., 1929, Proc. R. Soc. London, Ser. A **124**, 425.
Mott, N. F., 1932, Proc. R. Soc. London, Ser. A **135**, 429.
Mott, N. F. and H. S. W. Massey, 1965, *The Theory of Atomic Collisions* (Clarendon, Oxford).
Oppenheimer, J. R., 1927, Fortschr. Phys. **43**, 27.
Oppenheimer, J. R., 1929, Phys. Rev. **32**, 361.
Pachucki, K., 1998, J. Phys. B **31**, 2489, 3547.
Penney, W. G., 1932, Proc. Natl. Acad. Sci. USA **18**, 231.
Percival, I. C., and M. J. Seaton, 1958, Philos. Trans. R. Soc. London, Ser. A **251**, 113.
Rubin, K., B. Bederson, M. Goldstein, and R. E. Collins, 1969, Phys. Rev. **182**, 201.
Sapirstein, J., 1998, Rev. Mod. Phys. **70**, 55.
Schrödinger, E., 1926a, Ann. Phys. (Leipzig) **79**, 361, 489, 734.
Schrödinger, E., 1926b, Ann. Phys. (Leipzig) **80**, 437.
Schrödinger, E., 1926c, Ann. Phys. (Leipzig) **81**, 109.
Schrödinger, E., 1926d, Phys. Rev. **28**, 1049.
Schulz, G. J., 1963, Phys. Rev. Lett. **10**, 104.
Schulz, G. J., 1973, Rev. Mod. Phys. **45**, 378.
Schwartz, C., 1961, Phys. Rev. **123**, 1700.
Shore, B. W., 1967, Rev. Mod. Phys. **39**, 439.
Shull, G. G., C. T. Chase, and F. E. Meyers, 1943, Phys. Rev. **135**, 29.
Skinner, H. W. B., and E. T. S. Appleyard, 1927, Proc. R. Soc. A **117**, 224.
Slater, J. C., 1928, Phys. Rev. **32**, 339, 349.
Smith, K., 1966, Rep. Prog. Phys. **29**, 373.
Standage, M. C., and H. Kleinpoppen, 1976, Phys. Rev. Lett. **36**, 577.
Storry, C. H., and E. A. Hessels, 1998, Phys. Rev. A **58**, R8.
Thorsheim, H. R., J. Weiner, and P. Julienne, 1987, Phys. Rev. Lett. **58**, 2420.
Ulrich, M., *et al.*, 1998, in *Photonic, Electronic, and Atomic Collisions*, edited by F. Aumayr and H.-P. Winter (World Scientific, Singapore), p. 421.
Vane, C. R., S. Datz, H. F. Krause, P. F. Dittner, E. F. Deveney, H. Knudson, P. Grafstroem, R. Schuck, H. Gao, and R. Hutton, 1997, Phys. Scr. **73**, 167.

Wannier, G., 1953, Phys. Rev. **90**, 817.
Weingartshofer, A., J. K. Holmes, G. Candle, E. M. Clarke, and H. Krüger, 1977, Phys. Rev. Lett. **39**, 269.
Whelan, C. T., and H. R. J. Walters, 1997, Eds., *Coincidence Studies of Electron and Photon Impact Ionization* (Plenum, New York/London).
Yalim, H. A., D. Crejanovic, and A. Crowe, 1997, Phys. Rev. Lett. **79**, 2951.
Yamazaki, T., 1992, in *Atomic Physics 13*, Proceedings of the Thirteenth Internation Conference, Munich, 1992, edited by T. W. Hänsch, B. Neizer, and H.-O. Walther (AIP, New York), p. 325.
Yan, Z.-C., and G. W. F. Drake, 1998, Phys. Rev. Lett. **81**, 774.
Yang, C. N., 1948, Phys. Rev. **54**, 93.